Infrared spectroscopy of Pb layer growth on Si(111)

Annemarie Pucci,* Florian Kost, and Gerhard Fahsold
Kirchhoff Institute of Physics, University of Heidelberg, Im Neuenheimer Feld 227, 69120 Heidelberg, Germany

Mieczyslaw Jalochowski
Institute of Physics, University of M. Curie-Sklodowska, pl. M. Curie-Sklodowskiej 1, 20031 Lublin, Poland
(Received 9 June 2006; revised manuscript received 9 August 2006; published 29 September 2006)

The growth of Pb films on Si(111)-(6×6) Au and on Si(111)-(7×7) Au at 120 K was investigated *in situ* with infrared transmittance spectroscopy. In the development of the transmission spectra with film thickness the formation of the crystalline layer, the layer-by-layer growth mode, and size effects can be identified. The infrared spectra are analyzed with the Drude model for the dielectric function. In order to get a good fit, both the parameters' plasma frequency and relaxation rate must become thickness dependent, which is explained in relation to the quantum-size effects and to the classical-size effect. This work is the first infrared spectroscopic study of quantum-size effect-related oscillations in metal films.

DOI: 10.1103/PhysRevB.74.125428 PACS number(s): 78.20.−e, 78.30.−j, 73.50.−h, 78.67.−n

I. INTRODUCTION

Infrared (IR) spectroscopy is well established in studies of vibration modes in solid-state physics and surface science. It is also a powerful method for studies of free charge carriers, for example in ultrathin metal films.[1,2] In this paper IR transmittance spectroscopy is used as a contact-free method for conductivity studies of the system Pb on Si(111) during Pb deposition at 120 K. The system is well known for its size effects in the conductivity and for its phase transitions.[3–8] At lowest temperatures, the formation of an amorphous Pb layer on Si(111)-(7×7) was observed. At a critical thickness a structural phase transition takes place that we could detect also in IR transmittance because of the qualitative change of the dielectric function. The structural transition is correlated to the coalescence of islands with certain heights stabilized by the quantum-size effect (QSE).[9] Our scanning tunneling microscopy (STM) pictures from a separate study show very small islands below the transition and large terraces above the critical thickness. See Figs. 1(a) and 1(b). Pb deposited onto Si(111)-(6×6) Au substrate grows as a crystalline phase and in a layer-by-layer mode from the very beginning. Figure 1(c) shows 2.25 monolayers (ML) of Pb on an Si(111)-(6×6) Au substrate prepared under similar conditions as Fig. 1(a) and 1(b). On the flat Pb film an island forming the third monolayer is visible. Several isolated 2 ML thick islands are to be seen. Their presence is closely related to a growth modified by the QSE. If the temperature at film deposition approaches room temperature, the QSE-related double-layer growth mode is fully developed. The disordered growth phase is lacking for a Si(111)-(6×6) Au substrate, where the interaction between Pb and the Au-saturated surface is much stronger than between Pb and the clean Si surface. Hence, crystalline growth is forced from the very beginning. In the crystalline phase oscillations of the IR transmittance due to the QSE are observed. Surface scattering as the classical-size effect (CSE) contributes to all of the observed spectra and reveals the surface roughness development. As we will show here, both the effects, classical-size and quantum-size, influence the IR transmittance, which can be described by the thickness dependency of the plasma frequency and of the relaxation rate.

II. CONDUCTIVITY MODELS

A. Lead in the infrared

Up to wave numbers of at least 5000 cm^{-1} the middle-IR optical properties of lead can be well described with the Drude model for the dielectric function

$$\varepsilon(\omega) = \varepsilon_\infty - \frac{\omega_P^2}{\omega^2 + i\omega\omega_\tau} \tag{1}$$

with $\varepsilon_\infty = 1$ and the two Drude parameters' relaxation rate ω (i.e., inverse lifetime) and plasma frequency ω_P, both independent of circular frequency ω.[10,11] As a result of a fit to the dielectric function (obtained from IR reflectance of a polycrystalline sample via Kramers-Kronig transformation) for the range up to 10 000 cm^{-1} the parameters (in typical wavenumber units) are $\omega_\tau = \omega_{\tau,Bulk} = 1450$ cm^{-1} and $\omega_P = \omega_{P,Bulk} = 62\,000$ cm^{-1} at room temperature.[10] Assuming a linear dependency of the phonon scattering contribution to ω_τ on temperature, an extrapolation to 120 K gives a bulk relaxation rate $\omega_\tau = \omega_{\tau,Bulk} = 550$ cm^{-1} based on temperature-dependent dc resistivity data.[12] With the Fermi velocity $V_F = 1.83 \times 10^6$ m/s (Ref. 12) it follows the bulk mean free path $l_{mfp} \approx 18$ nm that is of the order of the information length $l_i = V_F 2\pi/\omega$ in the IR range of this study (i.e., 62 nm at 1000 cm^{-1}). Islands with bigger diameters give layerlike IR spectra. However, their boundaries may increase the relaxation rate. The IR transmittance decreases with average Pb thickness d, which is to the first order due to the increase of $d\omega\,\mathrm{Im}[\varepsilon] \propto d\sigma_{opt}$ (σ_{opt} is the IR optical conductivity). The two properties, average transmittance and spectral slope allow a precise determination of the two Drude parameters from a continuous metal film spectrum, if d is known from an independent measurement and if the pure substrate is well characterized.[1,13] It is important to note that the sensitivity of σ_{opt} to changes of the Drude parameters increases with decreasing ω, which is easily ascertainable by means of the corresponding derivatives of σ_{opt}.

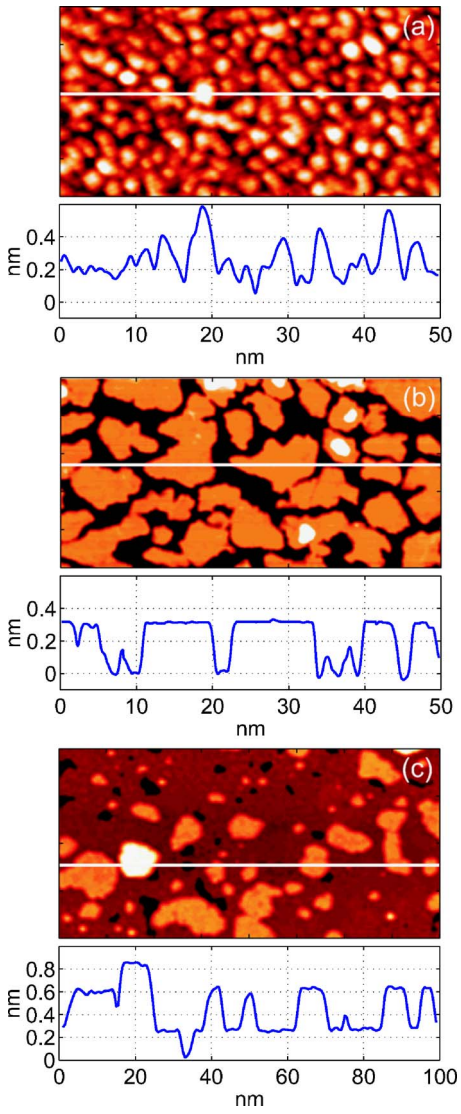

FIG. 1. (Color online) Topographical STM scans of Pb on Si(111)-(7×7) deposited and measured at 105 K under UHV conditions for Pb coverage of (a) 2.5 ML and (b) 6.5 ML, respectively, compared to respective scans of 2.25 ML of Pb deposited at 130 K onto Si(111)-(6×6) Au. The film (a) is amorphous-like; (b) with increasing thickness follows the transition into the crystalline phase. (c) The film is growing layer-by-layer from the beginning.

B. dc conductivity of Pb(111) films and size effect models

If renormalization effects[14] are negligible, the dc conductivity σ_{dc} should be equal to the low-frequency limit of $\sigma_{opt}(\omega \to 0) = \varepsilon_v \omega_P^2 / \omega_\tau$ (with the vacuum dielectric constant ε_v). For an ideal Fermi gas $\omega_P^2 = Ne^2/(m^* \varepsilon_v)$ with the electron density N, the electron charge e, and the effective electron mass m^*. For a real metal such simple relation does not work well and the plasma frequency follows from the band structure. For ultrathin (111) Pb layers Vilfan *et al.* calculated $\sigma_{dc}\omega_\tau$. Their result corresponds to a plasma frequency of about 59 000 cm^{-1} which is surprisingly close to the parameter from the middle IR and which coincides with the plasma frequency parameter obtained from a fit to data from the far IR. For example, in the case of iron, the discrepancy between optical and dc data is much bigger and a significant frequency dependence of ω_P has to be considered.[1,15]

For the thicker films of this study with thickness $d \gg \lambda_F$ (Fermi wavelength, it is 0.366 nm for the direction normal to Pb(111) layers) the CSE decreases the conductivity compared to the bulk. Following the work of Fuchs[16] and Sondheimer,[17] for the case of pronounced diffuse surface scattering, the thin-film relaxation rate becomes

$$\omega_\tau = \omega_{\tau,\mathrm{Bulk}} + \frac{3}{8}(1-p) v_F \frac{1}{d}, \tag{2}$$

with the probability p for specular scattering of free electrons. If surface roughness changes during film growth, it follows $p=p(d)$. Equation (2) assumes the independent scattering processes. Its applicability was proved many times. But for even thinner films, if the QSE comes into play, surface scattering is no more a simple additive contribution to the total relaxation rate. It depends explicitly on the subband quantum number n, see, for example, the following expression derived for the in-plane conductivity of a homogeneous film by Trivedi and Ashcroft.[18] In the presence of both "impurity" (point defect) scattering and surface scattering (in case of small-scale roughness, i.e., without grain boundary scattering) their theoretical in-plane conductivity, here expressed with the bulk parameters ω_P, $\omega_{\tau,\mathrm{Bulk}}$, and l_{mfp} ($\omega_{\tau,\mathrm{Bulk}}$ and l_{mfp} already accounting for impurity scattering), is

$$\sigma_{dc} = \frac{\omega_P^2 \varepsilon_v}{\omega_{\tau,\mathrm{Bulk}}} 3 \sum_{n=1}^{n_c} \frac{1 - n^2\pi^2 (k_F d)^{-2}}{2n_c + 1 + (\delta d/d)^2 k_F l_{mfp} s(n_c) n^2/3}; \tag{3}$$

the Fermi wave number is $k_F = 2\pi/\lambda_F$, with the root-mean-square deviation δd of the average film thickness d, $n_c = \mathrm{Int}[k_F d/\pi]$, and $s(n_c) = (n_c+1)(2n_c+1)/(2n_c^2)$. Equation (3) predicts oscillations of the conductivity and a slow approach to the bulk conductivity with increasing d. For sufficiently small δd, clear minima are expected for dk_F/π equal to an integer number. Surface roughness changes with thickness during Pb film growth, therefore $\delta d = \delta d(d)$. For an ideally smooth film and negligible diffuse surface scattering in Eq. (3), the bulk relaxation rate $\omega_{\tau,\mathrm{Bulk}}$ can be separated and the plasma frequency appears as modified by the QSE. Therefore, in the case of negligible surface scattering and island lateral dimensions larger than l_i, the parameter ω_P^2 obtained from a fit to IR spectra via Eq. (1) could be discussed in relation to $\sigma_{dc}\omega_{\tau,\mathrm{Bulk}}/\varepsilon_v$ from Eq. (3). However, Eq. (3) is valid only at a temperature $T=0$ and was derived under the assumption of a thickness-independent chemical potential.

III. EXPERIMENTAL

The experiments were performed in an ultra-high vacuum (UHV)-chamber that was equipped with a RHEED system and where the base pressure was 1×10^{-10} mbar (during Pb deposition about 7×10^{-10} mbar). The angle of the deposition direction to the Si surface normal was approximately 30° for Pb and for Au evaporation. The substrates were Si(111) wafers with about 10 Ω cm resistivity and the dimensions $20 \times 5 \times 0.375$ mm^3. They had been cleaned by using resistive dc heating and flashing up to about 1500 K for a

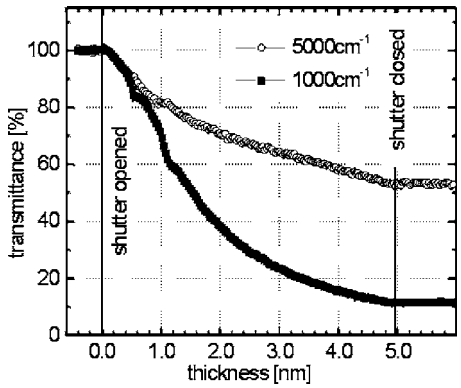

FIG. 2. Transmittance change (for the two wave numbers given) during Pb deposition on Si(111)-(6×6) Au. Deposition starts at 0 nm and is stopped at 5 nm.

few seconds. Hence, the oxide layer was removed and the Si(111)-(7×7) superstructure was produced, which has been monitored with the RHEED setup. Before lead deposition, the sample was cooled down to about 120 K by making thermal contact to a LN_2 cryostat. This temperature was measured with a Pt100 resistance thermometer. Lead was evaporated onto the cooled substrate by thermal evaporation at a rate of about 2.3 Å/min from an Al_2O_3 crucible. For the preparation of the Si(111)-(6×6) Au superstructure, before the lead deposition, 1.2 monolayers (ML) of gold were deposited onto Si(111)-(7×7) surface at room temperature (with a rate of about 0.4 Å/min) followed by annealing up to 700 °C and subsequent slow cooling down.

The metal deposition rates were calibrated by quartz microbalance measurements before and after each experiment. The average lead-film thickness (in nm) was calculated from the rate and the deposition time, using the bulk density of crystalline lead. The numbers of lead MLs are based on the lattice plane distance in the ⟨111⟩ direction: 1 ML =0.286 nm. The estimated relative error in Pb thickness is less than 10%.

The IR beam from the spectrometer (Bruker Tensor 27, N_2 purged) was lead into the UHV chamber by adjustable mirrors that focused the spot onto the sample. Using an aperture of 1 mm, the IR spot on the wafer had a diameter of about 1.8 mm. Regarding the IR data acquisition, each IR spectrum was measured with 20 scans and referred to the reference spectrum taken before lead deposition with 200 scans. The spectral resolution was 8 cm^{-1}. To avoid nonlinear effects in photon intensity measurements, a deuterated L-alanine-doped triglycene sulphate (DLATGS) detector was used. In order to get reasonable IR spectra during lead-film growth, it was particularly important to ensure high signal stability. To check the effect of our measures, a long-term IR measurement was performed to estimate the largest deviations. In the middle IR, for example, at 1000 cm^{-1} the directly (i.e., without any sample) transmitted intensity oscillates over a period of 15 h not much more than 0.5%.

The IR measurements take not longer than 0.5 h, and the measurements have demonstrated that the deviations during this time range up to a maximum of 0.03%. Fig. 2 reflects the signal stability with a cooled specimen, see the regions before and after closing the shutter, where the remaining deviations from constant transmittance are due to temperature fluctuations of the sample.

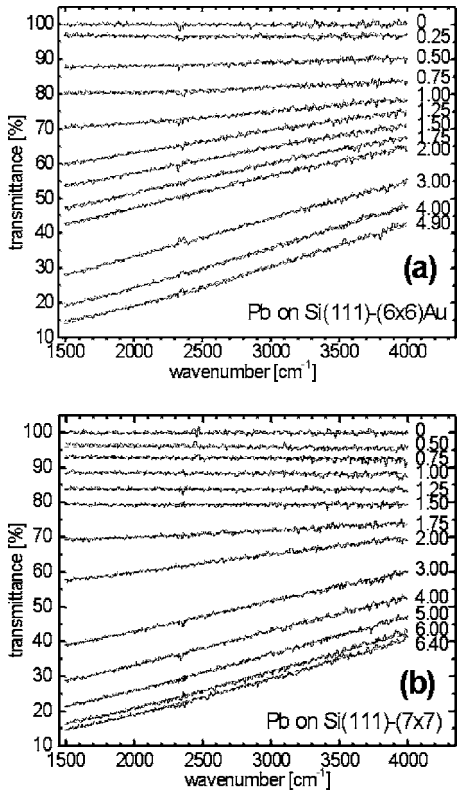

FIG. 3. Selection of relative transmittance spectra measured during Pb film growth at 120 K on (a) Si(111)-(6×6) Au and on (b) Si(111)-(7×7). The thickness for each spectrum is given in the figure. The broken lines that could hardly be distinguished from the experimental spectra (slightly noisy) are best-fit calculations based on the Drude model for the dielectric function.

IV. RESULTS

Figure 2 shows the time development of the transmittance during the growth of a lead film on a Si(111)-(6×6) Au surface versus Pb-film thickness. To gain a better signal-to-noise ratio, the transmittance values in Fig. 2 are average values for an interval of 100 cm^{-1} around the indicated wave number. For transmittance at 1000 cm^{-1}, minima can be seen at a thickness corresponding to 2 and 4 ML, whereas there are maxima for 5000 cm^{-1}. Supposed that the Drude model is valid; this finding indicates that ω_τ is equal to a circular frequency in the IR range in between.

A selection of spectra from 1500 cm^{-1} to 4000 cm^{-1} and the Drude-fit curves are shown in Fig. 3. The transmittance was calculated with the software package SCOUT[19] that exactly considers the thin-film optics. For the fits the Si-substrate transmittance was measured and described separately. In the fits to the film spectra that are based on Eq. (1), the two Drude parameters are treated as thickness-dependent (but frequency-independent) parameters. For d, the film thickness following from the deposition rate and deposition

time was used. It turned out that it was impossible to get a reasonable fit with only one thickness-dependent Drude parameter.

The IR spectra reveal the typical spectral behavior of a metal with high charge-carrier relaxation rate, i.e., the spectral slope is more or less linear with wave number, which is different for noble metals.[20,21] The comparison of the spectral development for both the substrates already makes obvious interesting differences that must be due to the different film structure, for example, compare transmittance for 0.5 nm which is much lower on the Si(111)-(6×6) Au surface.

Another peculiarity is the IR transmittance on the Si(111)-(7×7) surface below 1.5 nm. There is no obvious spectral change with frequency, which is a behavior typical for metal films near the percolation threshold[22] or for films with very high relaxation rates. Here, in the low thickness range, the optical conductivity seems to stay independent of both frequency and thickness and the transmittance decreases nearly linearly with average film thickness, which means that the film is growing in thickness but is not changing its electronic transport. This finding is in accordance with the STM result: the film is rather amorphous up to 4 ML.

For a more detailed discussion we look now on the development of the fit results for Drude parameters with thickness.

V. DISCUSSION

A. Pb on Si(111)-(6×6) Au

From the beginning of the Pb deposition onward, the fit based on Eq. (1) to the IR spectra at each thickness gives reasonable parameters: The obtained relaxation rate corresponds to a mean free path slightly bigger than the atomic radius up to 1 ML and drops down to values corresponding to a mean-free path of a few nm after the first ML is complete. The plasma frequency increases up to 1 ML and starts to oscillate above 1 ML. The most pronounced oscillations are shown in Fig. 4.

At 2 and 4 ML we see clear minima in the relaxation rate indicating a smooth surface. At 3 ML only a small dip in the relaxation rate indicating a flat surface could be seen. The minima at 2 and 4 ML in the squared plasma frequency would fit with the behavior of $\sigma_{dc}\omega_{\tau,Bulk}/\varepsilon_v$ according to Eq. (3) since there dk_F/π is an integer. But taking into account the thickness-dependent position of the chemical potential, we had to argue as follows.

The dominating double-layer periodicity in the IR transmittance is indeed caused mainly by electronic effects. In 2 and 4 ML of Pb on Si(111)-(6×6) Au the Fermi level is placed just between two quantum-size levels with roughly the same distance to Fermi level. In contrast, in 3, 5, and 7 ML the Fermi level is close to the respective quantum level. Accordingly, scattering is less in the first case (because of the smaller number of states available to scatter) and increases when a new QSE level is near the Fermi level, which is calculated in Refs. 23 and 24. Experimentally determined positions of the QSE levels are given in Ref. 25. Dips at 2 and 4 ML come from superposition of both the effects—the electronic one and the topographical one, where the electronic effect is prevailing. An explanation for plasma frequency variation is not clear. Minima suggest lower concentrations at 2 and 4 ML but this is not consistent with the distance of the quantum levels from the Fermi level at these thicknesses [lower concentration is expected when just a new QSE level crosses the Fermi level, see Eq. (3)]. However, we have to keep in mind that we have discussed this on the basis of a simplified one-dimensional model, but in fact, we deal with a much more complicated system.

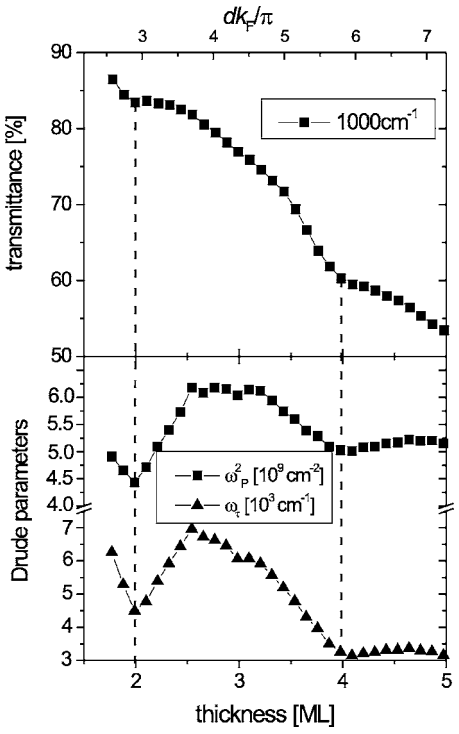

FIG. 4. Transmittance at 1000 cm^{-1} and Drude parameters versus Pb thickness given in ML and in bulk Fermi wavelengths (top scale). Substrate: Si(111)-(6×6) Au.

Figure 5 makes obvious that for Pb on Si(111)-(6×6) Au above 5 ML the average trend in relaxation rate corresponds to Eq. (2) with a nearly constant p. The linear extrapolation from $d^{-1}=(3\ \text{nm})^{-1}$ to $d^{-1}=0$ gives a bulk relaxation rate of about 250 cm^{-1}, which is half the value $\omega_{\tau,Bulk}$ for polycrystalline lead.

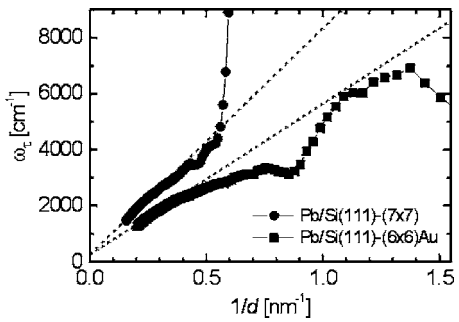

FIG. 5. Relaxation rates versus inverse Pb thickness $1/d$. The linear relationship at higher thickness d indicates the dominating CSE, its extrapolation is shown as a broken line.

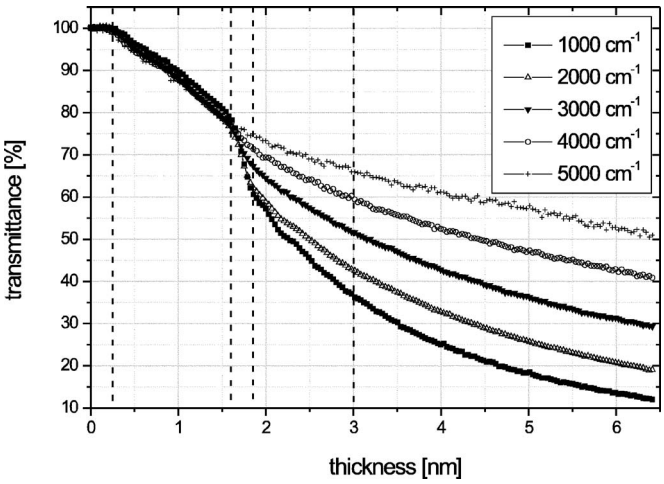

FIG. 6. Transmittance versus thickness for Pb on Si(111)-(7 $\times$7) showing the ordering transition above 1.7 nm. The five growth phases are separated with vertical broken lines.

B. Pb on Si(111)-(7×7)

On Si(111)-(7$\times$7) five different phases in the film formation can be distinguished. Up to approximately one ML, nearly no changes in the transmittance can be seen (see Fig. 6). The evaporated material has not yet sufficient influence on the conductivity, which corresponds to the formation of the wetting layer. Then, up to a film thickness of $\sim$1.7 nm, the transmittance is frequency-independent and decreases for all wave numbers nearly linearly with film thickness as mentioned above. Only beyond 1 nm Drude-type fits give physically reasonable values since then the relaxation rate ω_τ corresponds to a l_{mfp} above the Ioffe-Regel criterion ($l_{\mathrm{mfp}} > 1/k_{\mathrm{F}}$) for the existence of extended electronic wave functions.[26] At about 1.5 nm the relaxation rate reaches values that correspond to a mean free path similar to the atomic radius. Then a sudden drop down in transmittance is observed and a significant frequency dependence of transmittance develops, after which very slight signal oscillations occur, which are even more pronounced for lower wave numbers compared to the higher ones, see also Fig. 6. In the phase from approximately 3 nm to larger thicknesses, no oscillations can be detected anymore, but this region can be described by Eq. (2). Above 2.5 nm, because of the almost constant slope with $1/d$ (see Fig. 4) the specularity parameter p only negligibly changes with increasing thickness. Linear extrapolation from $1/d$=0.25 nm^{-1} to 0 gives a bulk relaxation rate of about 250 cm^{-1}.

For thickness above 1.5 nm, in the oscillation's region, the best-fit Drude parameters are shown in Fig. 7. Similarly, as in the case of Pb on Si(111)-(6$\times$6) Au (Fig. 4), the Drude parameters vary with the film thickness. Minima appear at about 6.4 ML ($\approx$1.8 nm) and, hardly to observe, at about 7.4 ML ($\approx$2.2 nm). As it follows from dc resistivity experiments on the same system, the QSE features are expected at an integer number of monolayers. Taking into account the experimental error of the thickness determination and looking at the existing knowledge on the system, we identify the position of the first minimum with the thickness of 6 ML and

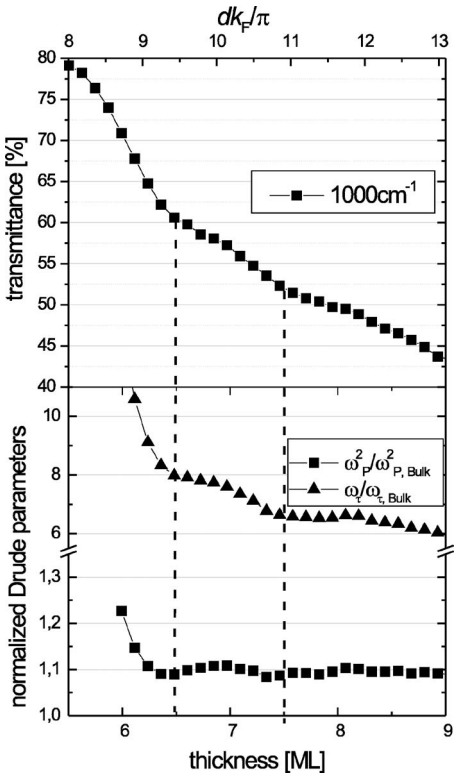

FIG. 7. Transmittance at 1000 cm^{-1} and Drude parameters (normalized to the bulk values given in Sec. II) versus Pb thickness given in ML and in bulk Fermi wavelengths (top scale). Substrate: Si(111)-(7$\times$7).

the second one with 7 ML. It should be noticed, that even higher accuracy and sensitivity in IR experiments is possible, but it would need a more elaborate (and more expensive) setup than the basic one used in this study.

Previous dc studies have confirmed the occurrence of two superimposed sets of resistivity oscillations in Pb ultrathin films.[3,24] The first set, with periodicity of 1 ML, results from the periodic modulation of scattering due to the oscillatory variation of surface roughness during layer-by-layer film growth. In a first approximation, without consideration of QSE, it can be described by Eq. (2) where the parameter p oscillates. One-ML resistance oscillations in ultrathin gold on Si(111)-(7$\times$7) at 95 K are the best example.[27] The second set, with 2 ML periodicity is described by Eq. (2), and results from QSE via modulation of charge-carrier density, surface, and defect scattering. dc resistivity experiments[23,24] proved that in Pb ultrathin epitaxial films the QSE is responsible for resistivity oscillation with 2 ML periodicity. In this study the QSE related features can be observed only after the mean free path of the charge carriers has become comparable to the thickness of the films. For Pb films deposited on Si(111)-(7$\times$7) this occurs after transformation into the crystalline phase at a thickness above 5 ML. Thus, oscillations of the Drude parameters can be observed only within a narrow window of thickness: from about 5 ML to about 10 ML; with increasing thickness the oscillation amplitude becomes increasingly small [Eq. (3) reflects such behavior]. The oscillations in the plasma frequency are much smaller than in the case of Pb on Si(111)-(6$\times$6) Au; d is already large and the

charge-carrier concentration already approaches a bulk value. The plasma frequency at higher thickness arrives for both sample types of this study at the IR bulk value roughly times 1.06, which should not be overestimated because of the uncertainty about the right bulk value.

VI. SUMMARY

This study demonstrates that IR spectroscopy is a powerful tool for the investigation of conductivity parameters of ultrathin metal films. Electric contacts are not necessary. The *in situ* IR spectroscopy allows the observation of the development of the film morphology and of the conductivity with metal thickness. The crystalline growth mode of lead on the Si(111)-(6×6) Au surface is confirmed and for the structural changes on the Si(111)-(7×7) surface, deeper insight is given into the correlated conductivity development. For higher thickness of a few nm and above, the surface scattering contribution and the bulk-limit data are derived. The bulk plasma frequency from this study is close to the literature value for the middle IR, but the difference to data for the dc case or low frequencies, respectively, shows, that renormalization indeed has some importance for comparison of dc and IR data. For the bulk relaxation rate it clearly follows a value for the crystalline Pb layers below the polycrystalline rate, indicating the low defect density of these films despite the relatively low deposition temperature of 120 K.

ACKNOWLEDGMENTS

Financial support for IR equipment for this work by the Deutsche Forschungsgemeinschaft (DFG) within priority program 1165 is gratefully acknowledged.

*Electronic address: pucci@kip.uni-heidelberg.de

[1] G. Fahsold, A. Bartel, O. Krauth, N. Magg, and A. Pucci, Phys. Rev. B **61**, 14108 (2000).
[2] P. F. Henning, C. C. Homes, S. Maslov, G. L. Carr, D. N. Basov, B. Nicolić, and M. Strongin, Phys. Rev. Lett. **83**, 4880 (1999).
[3] M. Jalochowski and E. Bauer, Phys. Rev. B **38**, 5272 (1988).
[4] I. Vilfan, M. Henzler, O. Pfennigstorf, and H. Pfnür, Phys. Rev. B **66**, 241306 (2002).
[5] O. Pfennigstorf, A. Petkova, H. L. Guenter, and M. Henzler, Phys. Rev. B **65**, 045412 (2002).
[6] K. A. Edwards, P. B. Howes, J. E. Mcdonald, T. Hibma, T. Bootsma, and M. A. James, Surf. Sci. **424**, 169 (1999).
[7] V. Yeh, L. Berbil-Bautista, C. Z. Wang, K. M. Ho, and M. C. Tringides, Phys. Rev. Lett. **85**, 5158 (2000).
[8] S. H. Chang, W. B. Su, W. B. Jian, C. S. Chang, L. J. Chen, and Tien T. Tsong, Phys. Rev. B **65**, 245401-1 (2002).
[9] K. Budde, E. Abram, V. Yeh, and M. C. Tringides, Phys. Rev. B **61**, R10602 (2000).
[10] M. A. Ordal, L. L. Long, R. J. Bell, S. E. Bell, R. R. Bell, R. W. Alexander, Jr., and C. A. Ward, Appl. Opt. **22**, 1099 (1983).
[11] M. A. Ordal, Robert J. Bell, R. W. Alexander, Jr., L. L. Long, and M. R. Querry, Appl. Opt. **24**, 4493 (1985).
[12] N. W. Ashcroft and N. D. Mermin, *Solid State Physics* (Saunders College Publishing, Orlando, 1976).
[13] G. Fahsold, M. Sinther, A. Priebe, S. Diez, and A. Pucci, Phys. Rev. B **65**, 235408 (2002).
[14] Chian-Yuan Young, J. Phys. Chem. Solids **30**, 2765 (1969).
[15] G. Fahsold and A. Pucci, in *Advances in Solid State Physics*, edited by B. Kramer (Springer, New York, 2003), Vol. 39, p. 833.
[16] K. Fuchs, Proc. Cambridge Philos. Soc. **34**, 100 (1938).
[17] E. H. Sondheimer, Adv. Phys. **1**, 1 (1952).
[18] N. Trivedi and N. W. Ashcroft, Phys. Rev. B **38**, 12298 (1988).
[19] Software SCOUT 2, M. Theiss, Hard- and Software for Optical Spectroscopy, Aachen, Germany.
[20] F. Meng, G. Fahsold, and A. Pucci, Phys. Status Solidi C **2**, 3963 (2005).
[21] A. Priebe, F. Meng, and A. Pucci, Asian J. Phys. **15**, 239 (2006).
[22] S. Berthier, J. Peiro, S. Fagnent, and P. Gadenne, Physica A **241**, 1 (1997).
[23] M. Jalochowski, E. Bauer, H. Knoppe, and G. Lilienkamp, Phys. Rev. B **45**, 13607 (1992).
[24] M. Jalochowski, M. Hoffmann, and E. Bauer, Phys. Rev. B **51**, 7231 (1995).
[25] M. Jalochowski, H. Knoppe, G. Lilienkamp, and E. Bauer, Phys. Rev. B **46**, 4693 (1992).
[26] D. C. Licciardello and D. J. Thouless, Phys. Rev. Lett. **35**, 1475 (1975).
[27] M. Jalochowski and E. Bauer, Phys. Rev. B **37**, 8622 (1988).